Dipolar Recoupling in MAS NMR: A Probe for Segmental Order in Lipid Bilayers

John D. Gross, Dror E. Warschawski, and Robert G. Griffin*

Contribution from the Francis Bitter Magnet Laboratory and Department of Chemistry, Massachusetts Institute of Technology, Cambridge, Massachusetts 02139

Received August 22, 1996[⊗]

Abstract: Novel two-dimensional magic-angle spinning (2D MAS) NMR experiments designed to measure the magnitudes and signs of $^{13}C-^{1}H$ dipolar interactions in fluid phase lipid bilayers are presented. MAS is employed throughout the experiments while dipolar recoupling is achieved (by radio frequency irradiation) during the evolution period. Multiple $^{13}C-^{1}H$ dipolar couplings are measured for a natural abundance sample of L_α phase dimyristoylphosphatidylcholine (DMPC). The magnitudes of $^{13}C-^{1}H$ dipolar interactions are determined by fitting numerical simulations of recoupled powder line shapes with experimental data while the signs of these interactions are obtained by monitoring the buildup of antiphase magnetization by ^{13}C detection. A comparison of the order parameters obtained by $^{13}C-^{1}H$ dipolar recoupling with those previously obtained for DMPC by ^{2}H NMR indicates that dipolar recoupling is a viable method for determining segmental order in fluid phase lipid bilayers without recourse to isotopic enrichment. Measurement of the signs of $^{13}C-^{1}H$ dipolar couplings provides additional structural information that is unavailable through ^{2}H NMR. The results obtained for DMPC suggest that the accuracy of the dipolar recoupling experiments presented in this work is competitive with that of previous techniques which require switched-angle spinning for the measurement of the magnitudes and signs of $^{13}C-^{1}H$ dipolar interactions in lipid bilayers.

Introduction

Over the last two decades, ^{2}H NMR has been an important method for investigating the structure and dynamics of liquid crystalline systems such as lipid bilayers.[1−3] The ^{2}H quadrupolar coupling provides an excellent probe of $C-^{2}H$ (CD) segmental order since the quadrupolar tensor is, in general, axially symmetric, with the unique axis directed along the CD bond.[4] In randomly oriented samples containing a specifically labeled CD segment, the quadrupolar coupling is obtained by measuring the width of a Pake doublet. A departure from the 250 kHz rigid lattice width is indicative of motions (*vide infra*), and the powder line shape contains information regarding the average orientation of the CD segment with respect to the motional axis.[1,3] Furthermore, ^{2}H Pake patterns provide a useful mapping of orientation dependent relaxation. Simulations of both T_1[5−7] and T_2[2,8−10] anisotropy have yielded excellent models of lipid dynamics in both gel and fluid phases.

A major shortcoming of ^{2}H NMR is the requisite isotopic enrichment, due to a prohibitively low natural abundance (0.01%), for the measurement of spectra. Therefore, there has been an increased interest in obtaining similar information from directly bonded $^{13}C-^{1}H$ dipolar couplings[11−16] since the spatial dependence of the $^{13}C-^{1}H$ dipolar tensor is formally identical to that of the ^{2}H electric field gradient tensor and it is possible to record natural abundance ^{13}C spectra in concentrated samples such as liquid crystals. In contrast to ^{2}H NMR, where the quadrupolar coupling dominates other spin interactions such as dipolar couplings and chemical shifts, interpretation of $^{13}C-^{1}H$ dipolar splittings may be complicated by chemical shift anisotropy (CSA) and dipolar interactions among abundant spins. In addition, multiple $^{13}C-^{1}H$ dipolar couplings found in more complicated systems make ^{13}C spectra difficult to disentangle. The latter complication is partially solved by separated-local-field spectroscopy on static samples where dipolar interactions and chemical shifts are separated into orthogonal frequency domains in a 2D experiment. There, each magnetically distinct site, defined by a unique chemical shift, reports on the individual dipolar fields,[17] and multiple $^{13}C-^{1}H$ couplings are resolved by their associated ^{13}C chemical shift.

The first separated-local-field experiments were performed with static single crystalline solids, but unfortunately, powder samples generate additional broadening that reduces sensitivity with a concomitant loss of resolution.[17] The advent of cross polarization with magic-angle spinning (CP/MAS)[18] and high power proton decoupling has dramatically increased the sensitivity and resolution in spectra of rare nuclei such as ^{13}C. Indeed, isotropic chemical shift spectra rivaling the quality of resolution obtained in liquids may be recorded for solids but at the sacrifice of orientation dependent information. It was

[⊗] Abstract published in *Advance ACS Abstracts,* January 1, 1997.

(1) Seelig, J.; Seelig, A. *Q. Rev. Biophys.* **1980**, *13*, 19−61.
(2) Davis, J. H. *Biochim. Biophys. Acta* **1983**, *737*, 117−171.
(3) Spiess, H. W. *Adv. Polym. Sci* **1985**, *66*, 23.
(4) Oldfield, E.; Chapman, D.; Derbyshire, W. *FEBS Lett.* **1971**, *16*, 103−104.
(5) Siminovitch, D. J.; Olejniczak, E. T.; Ruocco, M. J.; Gupta, S. K. D.; Griffin, R. G. *Chem. Phys. Lett.* **1985**, *119*, 251.
(6) Wittebort, R. J.; Olejniczak, E. T.; Griffin, R. G. *J. Chem. Phys.* **1987**, *86*, 5411−5420.
(7) Speyer, J. B.; Weber, R. T.; Gupta, S. K. D.; Griffin, R. G. *Biochemistry* **1989**, *28*, 9569−9574.
(8) Spiess, H. W.; Sillescu, H. *J. Magn. Reson.* **1981**, *42*, 381−389.
(9) Blume, A.; Griffin, R. G. *Biochemistry* **1982**, *24*, 6230−6242.
(10) Mayer, C.; Muller, K.; Weisz, K.; Kothe, G. *Liq. Cryst.* **1988**, *3*, 797−806.
(11) Munowitz, M.; Griffin, R. G.; Bodenhausen, G.; Huang, T. H. *J. Am. Chem. Soc.* **1981**, *103*, 2529.
(12) Schaefer, J.; Stejskal, E. O.; McKay, R. A.; Dixon, W. T. *J. Magn. Reson.* **1983**, *52*, 123−129.
(13) Terao, T.; Miura, H.; Saika, A. *J. Chem. Phys.* **1986**, *85*, 3816−3826.
(14) Kolbert, A. C.; Levitt, M. H.; Griffin, R. G. *J. Magn. Reson.* **1989**, *85*, 42−49.
(15) Sanders, C. R.; Prestegard, J. H. *J. Am. Chem. Soc.* **1991**, *113*, 1987−1996.
(16) Nakai, T.; Terao, T. *Magn. Reson. Chem.* **1992**, *30*, 42−44.
(17) Hester, K.; Ackerman, J. L.; Neff, B. L.; Waugh, J. S. *Phys. Rev. Lett.* **1976**, *36*, 1081−1083.
(18) Schaefer, J.; Stejskal, E. O. *J. Am. Chem. Soc.* **1976**, *98*, 1031.

S0002-7863(96)02951-4 CCC: $14.00

precisely within this framework that Munowitz and co-workers proposed the idea of selectively re-introducing anisotropic interactions during MAS.[11] The dipolar-chemical shift correlation (DIPSHIFT) experiment is a MAS analog of the separated-local-fields experiment of Hester et al.[17] A notable increase in sensitivity and resolution is achieved since the powder patterns present in the evolution and detection period are replaced with rotational sidebands. Analysis of the dipolar sideband intensities yields the magnitude of $^{13}C-^{1}H$ dipolar couplings provided that the sample spinning speed is less than the $^{13}C-^{1}H$ dipolar interactions,[19] a condition that is generally satisfied for directly bonded $^{13}C-^{1}H$ couplings in rigid solids. However, in weakly coupled spin pairs, such as $^{13}C-^{13}C$ and $^{13}C-^{15}N$, it is difficult to obtain significant sideband intensity at typical spinning speeds. Methods that increase the number of spinning sidebands by magnifying the effective dipolar interactions during the dipolar evolution period[20−22] require slow spinning and, in general, the CSAs of multiple sites may overlap, thereby complicating spectral analysis. Alternatively, methods that involve the dephasing of rotational echoes, such as rotational echo double resonance (REDOR),[23] are not restricted by slow spinning and have consequently found wide use in measuring the magnitudes and signs[24] of weak couplings among rare spin nuclei. In the opposite regime, where dipolar couplings become large relative to experimentally realizable spinning speeds, the REDOR experiment becomes difficult to implement since the spectral window that accommodates dipolar powder patterns is limited by the spinning speed.[23]

Unlike in rigid solids, directly bonded $^{13}C-^{1}H$ dipolar couplings in liquid crystalline systems such as lipid bilayers may range from the order of 1 to 10 kHz. Such motionally averaged dipolar interactions are in the intermediate range with respect to spinning speeds typically employed. Although the larger couplings within this range could be measured with the DIPSHIFT[11] type of experiment while the weaker couplings could be measured with REDOR[23] or frequency selective dipolar recoupling (FDR),[25] clearly it would be beneficial to measure a range of dipolar couplings within one experiment. Techniques that allow scaling control of anisotropic interactions while preserving the recoupled powder line shape relative to the shape of the static line are a desirable means to this end. Uniform scaling of recoupled interactions may be achieved by switching either the angle of rotation[13,26] or the spinning speed[27,28] between dipolar evolution and detection periods; however, these techniques require specialized hardware and are difficult to implement.

We present here recoupling techniques for the measurement of both the magnitudes and signs of motionally averaged $^{13}C-^{1}H$ interactions found in liquid crystalline systems. The approach utilizes MAS at a constant speed throughout the experiment while a series of rotor-synchronized π pulses is applied for $^{13}C-^{1}H$ dipolar recoupling during the evolution period. Spacing between π pulses may be varied in order to control scaling of the recoupled Pake patterns, ensuring the simultaneous measurement of a wide range of couplings with an orientation dependence of the recoupled dipolar interactions that is identical to that of static samples. The methods introduced here are therefore π pulse analogs of the switched-angle spinning experiments previously proposed for the measurement of the magnitudes[13,16] and signs[29,30] of $^{13}C-^{1}H$ dipolar interactions. Accordingly, these experiments are referred to as DROSS (Dipolar Recoupling On-axis with Scaling and Shape preservation) and S-DROSS (Sign-DROSS) for the measurement of the magnitudes and signs of dipolar interactions. Their applicability is restricted to a class of systems where fast limit molecular motion enables $^{1}H-^{1}H$ dipolar couplings to be effectively averaged by MAS. However, this class includes a large number of chemically, physically, and biologically important systems such as model membranes and other liquid crystals which have heretofore relied almost exclusively on ^{2}H labeling for the study of segmental order.

Theory

Fast Limit Motional Averaging and the Effects on MAS Dynamics. There are considerable large amplitude molecular motions in fluid phase lipid bilayers. It is well-known that both gauche-trans isomerization and axial diffusion are rapid relative to $^{1}H-^{1}H$ and $^{13}C-^{1}H$ dipolar time scales, and consequently these anisotropic interactions are attenuated relative to their rigid lattice values.[31,32] Rapid axial motion, as demonstrated by Oldfield et al.[33] and Forbes et al.,[34] and recently discussed in detail by Davis,[35] enables MAS to effectively average ^{1}H homonuclear dipolar couplings. This is a remarkable result which indicates that high-resolution ^{1}H spectra may be obtained with MAS since the broadening off of rotational-resonance[36,37] is negligible in fluid phase lipid bilayers even at moderate spinning speeds.[35] In the language of Maricq and Waugh, the total Hamiltonian may be viewed as inhomogeneous under these conditions.[36] Therefore, $^{13}C-^{1}H$ dipolar couplings may be treated as independent spin pairs, and the relevant rotating frame Hamiltonian for a rare spin $^{1}/_{2}$ nucleus, S, in the presence of abundant spin $^{1}/_{2}$ nuclei, I, under MAS reduces to

$$H(t) = \langle\omega_I(t)\rangle I_z + \langle\omega_S(t)\rangle S_z + \langle\omega_{IS}(t)\rangle 2I_zS_z \qquad (1)$$

where the expressions $\omega_I(t)$, $\omega_S(t)$, and $\omega_{IS}(t)$ correspond to the I spin chemical shift, the S spin chemical shift, and heteronuclear couplings between spins I and S under MAS.[36] The broken brackets indicate motional averaging over time scales that are short relative to the MAS period.[38]

Pulse Sequences for Measuring the Magnitudes and the Signs of CH Dipolar Couplings. The pulse sequences for measuring the magnitude and the sign of CH dipolar couplings are depicted in Figure 1, parts a and b. Dipolar recoupling is achieved through an adaptation of the rotor-synchronized CSA

(19) Munowitz, M. G.; Griffin, R. G. *J. Chem. Phys.* **1982**, *76*, 2848.
(20) Gullion, T.; Poliks, M. D.; Schaefer, J. *J. Magn. Reson.* **1988**, *80*, 553−558.
(21) Bork, V.; Gullion, T.; Hing, A.; Schaeffer, J. *J. Magn. Reson.* **1990**, *88*, 523−532.
(22) Kolbert, A. C.; Griffin, R. G. *J. Magn. Reson.* **1991**, *93*, 242−255.
(23) Gullion, T.; Schaefer, J. *J. Magn. Reson.* **1989**, *81*, 196−200.
(24) Hing, A. W.; Schaefer, J. *Biochemistry* **1993**, *32*, 7593−7604.
(25) Bennett, A. E.; Rienstra, C. M.; Lansbury, P. T., Jr.; Griffin, R. G. *J. Chem. Phys.* **1996**, *105*, 10289−10299.
(26) Bax, A.; Szeverenyi, N. M.; Maciel, G. E. *J. Magn. Reson.* **1983**, *55*, 494−497.
(27) Zeigler, R. C.; Wind, R. A.; Maciel, G. E. *J. Magn. Reson.* **1988**, *79*, 299−306.
(28) Kolbert, A. C.; Groot, H. J. M. D.; Griffin, R. G. *J. Magn. Reson.* **1989**, *85*, 60−68.
(29) Hong, M.; Schmidt-Rohr, K.; Pines, A. *J. Am. Chem. Soc.* **1995**, *117*, 3310−3311.
(30) Hong, M.; Schmidt-Rohr, K. *J. Magn. Res. B* **1995**, *109*, 284−290.
(31) Bloom, M.; Burnell, E. E.; Roeder, S. B. W.; Valic, M. I. *J. Chem. Phys.* **1977**, *66*, 3012−3020.
(32) Bloom, M.; Burnell, E. E.; Mackay, A. L.; Nichol, C. P.; Valic, M. I.; Weeks, G. *Biochemistry* **1978**, *17*, 5750−5762.
(33) Oldfield, E.; Meadows, M.; Rice, D.; Jacobs, R. *Biochemistry* **1978**, *17*, 2727−2740.
(34) Forbes, J.; Bowers, J.; Moran, L.; Shan, X.; Oldfield, E. *J. Chem. Soc., Faraday Trans.* **1988**, *84*, 3821−3849.
(35) Davis, J. H.; Auger, M.; Hodges, R. S. *Biophys. J.* **1995**, *69*, 1917−1932.
(36) Maricq, M. M.; Waugh, J. S. *J. Chem. Phys.* **1979**, *70*, 3300−3316.
(37) Levitt, M. H.; Raleigh, D. P.; Creuzet, F.; Griffin, R. G. *J. Chem. Phys.* **1990**, *92*, 6347−6364.
(38) Torchia, D. A.; Szabo, A. *J. Magn. Reson.* **1982**, *49*, 107−121.

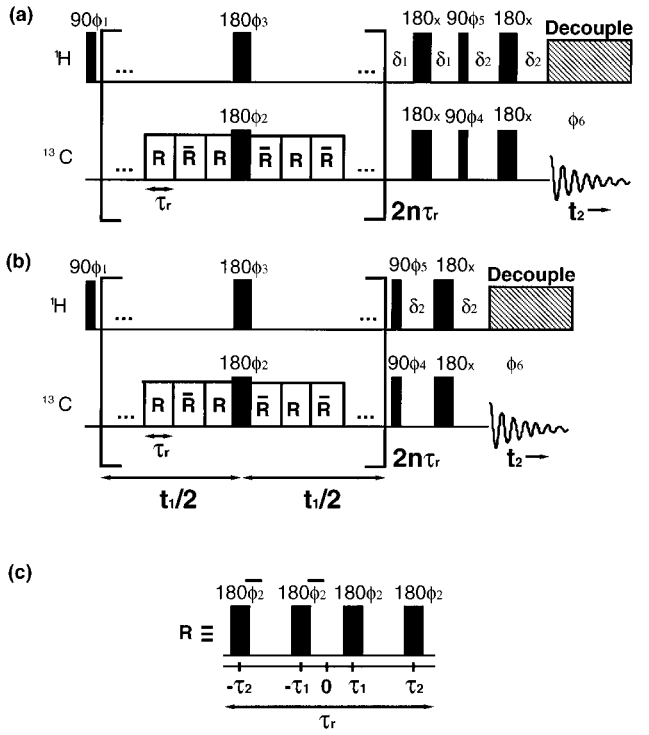

Figure 1. Pulse sequences for measuring the magnitudes and signs of dipolar interactions under MAS and the 4-π pulse recoupling scheme: (a) 2D DROSS, (b) S-DROSS, and (c) 4-π pulse recoupling scheme. Selected values of the scaling factors χ and ϵ with the corresponding pulse spacings given by $\omega_r\tau_1/2\pi$ and $\omega_r\tau_2/2\pi$ are tabulated in ref 39. Delays δ_1 and δ_2 are integer multiples of the rotor period and are either set equal to values of $^1/_4J_{CH}$ and $^1/_8J_{CH}$ or optimized empirically. Phase cycling for 2D DROSS (a): $\phi_1 = (xxyy)$, $\phi_2 = \phi_4 = (x\bar{x}y\bar{y})$, $\phi_3 = (yy\bar{x}\bar{x})$-$(\bar{y}\bar{y}xx)$, $\phi_5 = (yy\bar{x}\bar{x})$, $\phi_6 = (x\bar{x}y\bar{y})(\bar{x}xy\bar{y})$. Phase coupling for S-DROSS (b): $\phi_1 = (xxyy)(\bar{x}\bar{x}y\bar{y})$, $\phi_2 = (xy\bar{x}\bar{y})$, $\phi_3 = (xy\bar{x}\bar{y})$, $\phi_4 = (x\bar{x}y\bar{y})$, $\phi_5 = (y\bar{y}\bar{x}x)$, $\phi_6 = (x\bar{x}y\bar{y})(\bar{x}x\bar{y}y)$.

recoupling sequence suggested by Tycko et al. (see Figure 1c).[39] In both sequences, the heteronuclear dipolar interactions and S spin CSA are recoupled during both halves of the evolution period. However, the simultaneous π pulses on ^{1}H and ^{13}C, applied at the center of the evolution period, ensure that the chemical shifts are refocused over the duration of t_1. Therefore, evolution of initial transverse magnetization is governed by the effective Hamiltonian:

$$H^{\text{eff}} = \overline{\langle\omega_D\rangle}\, 2I_zS_z \tag{2}$$

where

$$\overline{\langle\omega_D\rangle} = \epsilon\pi J_{\text{CH}} + \chi\langle b_{\text{CH}}\rangle\frac{1}{2}(3\cos^2\beta - 1) \tag{3}$$

with β as the angle between the bilayer normal and the direction of the static magnetic field and

$$\langle b_{\text{CH}}\rangle = -b_{\text{CH}}S_{\text{CH}} \tag{4}$$

as the motionally averaged heteronuclear dipolar coupling, where

$$S_{\text{CH}} = \frac{1}{2}\langle 3\cos^2\theta - 1\rangle \tag{5}$$

is the ^{13}C$-^1$H dipolar order parameter, $b_{\text{CH}} = (\mu_0/4\pi)(\gamma_c\gamma_h\hbar/r_{\text{CH}}^3)$ is the rigid lattice dipolar coupling, and θ is the average angle between the internuclear vector and motional axis. The spacings τ_1 and τ_2 corresponding to several values of the scale factors χ and ϵ (ranging from 0 to 0.393 and from 0.797 to 0, respectively) are tabulated in ref 39.

In principle, the DROSS experiments could be implemented with the 4-π pulse sequence applied to either ^{13}C or the ^{1}H nuclei; however, it is found experimentally that the later case yields distorted line shapes. Numerical line shape simulations that include the effect of finite π pulses and homonuclear dipolar couplings between protons indicate decreasing line shape distortions with increasing power. In the limit of δ-function π pulses ideal Pake patterns are recovered. The effect is unobservable when ^{1}H dipolar couplings are neglected. In contrast, the effects of finite pulses on the rare spins are minimal for the radio frequency field strengths and resonance offsets employed in this work. Therefore, the 4-π pulse recoupling scheme is applied to the ^{13}C nuclei.

In addition, the techniques presented here could be performed by employing either ^{13}C or ^{1}H transverse magnetization as an initial condition for the evolution period. Although the former case would not require coherence transfer from ^{1}H to ^{13}C, evolution of ^{13}C magnetization under recoupled ^{13}C$-^1$H dipolar couplings would complicate spectral line shapes. In analogy to the J_{CH} coupling in liquids, a CH group yields a doublet while CH_2 and CH_3 moieties generate ^{13}C$-^1$H dipolar "triplets" and "quartets". In contrast, an initial condition of ^{1}H transverse magnetization generates doublets irrespective of ^{1}H multiplicity since each ^{1}H in the CH_n group is coupled to only one ^{13}C thereby simplifying spectral analysis. Accordingly, ^{1}H transverse magnetization is allowed to evolve under the recoupled ^{13}C$-^1$H dipolar interaction in both experiments.

In the 2D DROSS experiment, after a time t_1, the resulting proton magnetization is transferred in an orientation-independent fashion via J_{CH} to the directly bonded ^{13}C with a rotor-synchronized refocused-INEPT.[40,41] The resulting ^{13}C magnetization, $S_x\cos(\overline{\langle\omega_D\rangle}t_1)$, then evolves under MAS with proton decoupling. A two-dimensional Fourier transform generates a 2D DROSS spectrum where scaled, recoupled powder line shapes are separated by the corresponding ^{13}C chemical shifts.

For the case of S-DROSS, omission of the first refocusing period, $2\delta_1 = {}^1/_2J_{\text{CH}}$, found in the DROSS sequence ensures that the simultaneous $\pi/2$ pulses select and transfer proton antiphase magnetization, $2I_yS_z$, carrying the $\sin(\overline{\langle\omega_D\rangle}t_1)$ term to net ^{13}C magnetization on the directly bonded carbon during the subsequent delay. Just as in the switched-angle spinning version of the experiment,[29,30] the sign of the $\sin(\overline{\langle\omega_D\rangle}t_1)$ term, resulting from a ^{13}C$-^1$H dipolar coupling during the evolution time t_1, determines the sign of the corresponding ^{13}C resonance. That is, for short evolution times relative to the inverse of the recoupled dipolar coupling, the sign of the resulting ^{13}C resonance is determined by $\chi\langle\pm\omega_D\rangle t_1$, provided that $|\chi\langle\pm\omega_D\rangle| \gg \epsilon\pi J_{\text{CH}}$. A series of one-dimensional spectra are collected for different values of t_1 so that the initial buildup rate of ^{1}H antiphase magnetization may be monitored. Alternatively, the signs may be extracted from the polarity of antiphase Pake doublets resulting from a 2D implementation.

Materials and Methods

Sample Preparation. Dimyristoylphosphatidylcholine (DMPC) was purchased from Avanti Polar Lipids (Alabaster, AL) as a solution in chloroform and used without further purification. Samples were

(39) Tycko, R.; Dabbagh, G.; Mirau, P. A. *J. Magn. Reson.* **1989**, *85*, 265−274.
(40) Burum, D. P.; Ernst, R. R. *J. Magn. Reson.* **1980**, *39*, 163−168.
(41) Gross, J. D.; Costa, P. R.; Dubacq, J.-P.; Warschawski, D. E.; Lirsac, P.-N.; Devaux, P. F.; Griffin, R. G. *J. Magn. Reson. B* **1995**, *106*, 187−190.

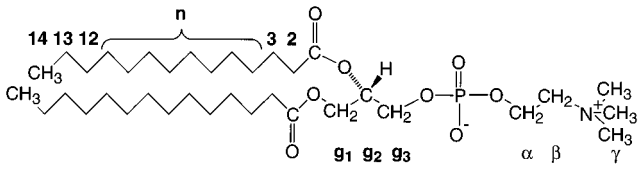

Figure 2. Schematic representation of DMPC.

prepared by evaporating chloroform under a gentle stream of N_2 followed by mechanical vacuum pumping overnight. Dispersions of DMPC in D_2O with a 1:1 ratio by weight were subjected to three freeze−thaw cycles before performing NMR experiments.

NMR Methods. All NMR experiments were performed on a custom designed spectrometer operating at a proton frequency of 397.9 MHz. Spectra were recorded with a custom designed double tuned probe equipped with a 5 mm high-speed spinning assembly procured from Doty Scientific, Inc (Columbia, SC). Spinning speeds were 8.0 kHz and controlled to within 2 Hz with a Doty spinning speed controller while the sample temperature was maintained at 30 °C throughout the experiment. Typical $\pi/2$ pulse lengths were 4.0 and 4.4 μs for ^{1}H and ^{13}C, respectively. Proton decoupling during the acquisition period was achieved using the two-pulse phase modulation scheme[42] with a radio frequency field strength of 50 kHz, a pulse length of 10.4 μs, and a phase angle ϕ of 10°. The 2D experiments were acquired with 512 scans per t_1 point and a recycle delay of 3 s. Quadrature detection during the evolution period was omitted due to the symmetry of the dipolar interaction. The data matrices, originally 32 × 1024 points, were zero filled to 128 × 2048 points. Data were processed with a sinebell window function in t_2 and 50−100 Hz Gaussian multiplication in t_1 prior to Fourier transformation.

Numerical Line Shape Simulations. In order to extract information on orientational order from the spectra, it is necessary to simulate the recoupled powder line shapes. Accordingly, the spin dynamics of an isolated CH or CH_2 segment during MAS and the 4-π pulse recoupling sequence, including finite pulse effects, were evaluated by numerical integration of the propagator. For simplicity, the coherence transfer from ^{1}H to ^{13}C is neglected so that only the propagator for the evolution period is calculated. The amplitude modulated ^{1}H magnetization is then Fourier transformed to generate powder line shapes. The principal values for the ^{1}H and ^{13}C chemical shift tensors in polyethylene[43,44] were employed in the simulations. In general it was found that ≥5000 orientations were needed for convergence of the powder average.

The simultaneous π pulses in the center of the evolution period complicate the numerical evaluation of the propagator. For exact calculations including these pulses, the amplitude of ^{1}H transverse magnetization would be found by forming the propagator for each value of t_1 which would be time consuming. A significant increase in computational speed is realized if the simultaneous π pulses are neglected, and the resulting periodicity of the 4-π pulse scheme is fully exploited. For the radio frequency power levels and resonance offsets employed, there is excellent agreement between exact (involving simultaneous π pulses) and approximate (neglecting simultaneous π pulses and setting ^{1}H resonance offsets and CSAs to zero) simulations where the propagator is calculated only once. Therefore, such approximate simulations are employed in this work unless mentioned otherwise.

Results and Discussion

A 2D DROSS spectrum of DMPC at 30 °C is depicted in Figure 3 for $\chi = 0.393$ and $\epsilon = 0.0$. Pake doublets are obtained since the 4-π pulse scheme of Tycko et al.[39] preserves the recoupled powder line shape: the angular dependence of the recoupled dipolar interaction is identical to that for static samples. Moreover, the 2D DROSS experiment may be employed with smaller values of χ if additional scaling is required.[39] In analogy with off magic-angle spinning (where

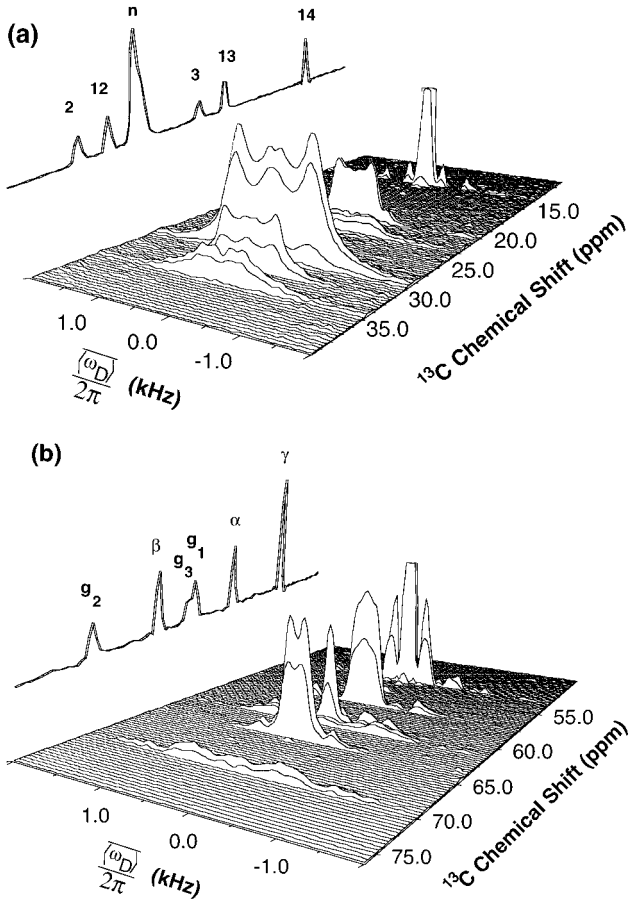

Figure 3. 2D ^{13}C−^{1}H DROSS spectrum of DMPC: (a) acyl chain region and (b) head group and glycerol region. The values of $\omega_r\tau_1/2\pi$ and $\omega_r\tau_2/2\pi$ chosen were 70.9° and 160.9° which correspond to $\chi = 0.393$ and $\epsilon = 0.0$. The delays δ_1 and δ_2 where set to 1.5 and 1.0 ms, respectively. The powder line shapes corresponding to C_{14} and γ contain artifacts arising from data truncation during the evolution period.

the angle between the spinner axis and the static magnetic field, Θ, may be varied to generate a desired scaling of the recoupled interactions by $P_2(\cos\Theta)$[13]), the pulse spacings τ_1 and τ_2 may be varied to give a specified scaling of χ without deviating from the magic-angle.[39]

The CH_2 and CH_3 groups found in DMPC contain at least two ^{13}C−^{1}H dipolar couplings which *a priori* need not be identical. However, from ^{2}H NMR on specifically labeled CD_2 and CD_3 lipid bilayers it is well-known that fast limit gauche-trans isomerization and axial diffusion renders the CD tensors, and therefore CH dipolar tensors, identical so that only one splitting is observed for most sites. The powder patterns found in Figure 3 mirror the line shapes observed in ^{2}H NMR with the exception of the small central splittings which are attributed to long-range ^{13}C−^{1}H dipolar couplings. For example, the top row of Figure 4a depicts several recoupled dipolar powder patterns taken from the g_2, C_{12}, and α positions of the 2D DROSS spectrum. The C_{12} and α positions, which are CH_2 groups, both contain only two splittings with the larger splitting corresponding to the value given by ^{2}H NMR for the motionally equivalent CH sites. Similar results are obtained for the C_{13} and β sites (data not shown). As expected, the g_2 site contains only one large splitting since it is a CH group. In contrast, methylene segments closer to the bilayer interface, such as the glycerol backbone and the upper region of the acyl chains, are more motionally restricted and are known to contain inequivalent sites. For example, one of the CH segments in the g_1 CH_2 group is dynamically averaged so that the angle between the motional

(42) Bennett, A. E.; Rienstra, C. M.; Auger, M.; Lakshmi, K. V.; Griffin, R. G. *J. Chem. Phys.* **1995**, *103*, 6951−6958.
(43) Burum, D. R.; Rhim, W.-K. *J. Chem. Phys.* **1979**, *71*, 944.
(44) Nakai, T.; Ashida, J.; Terao, T. *J. Chem. Phys.* **1988**, *88*, 6049.

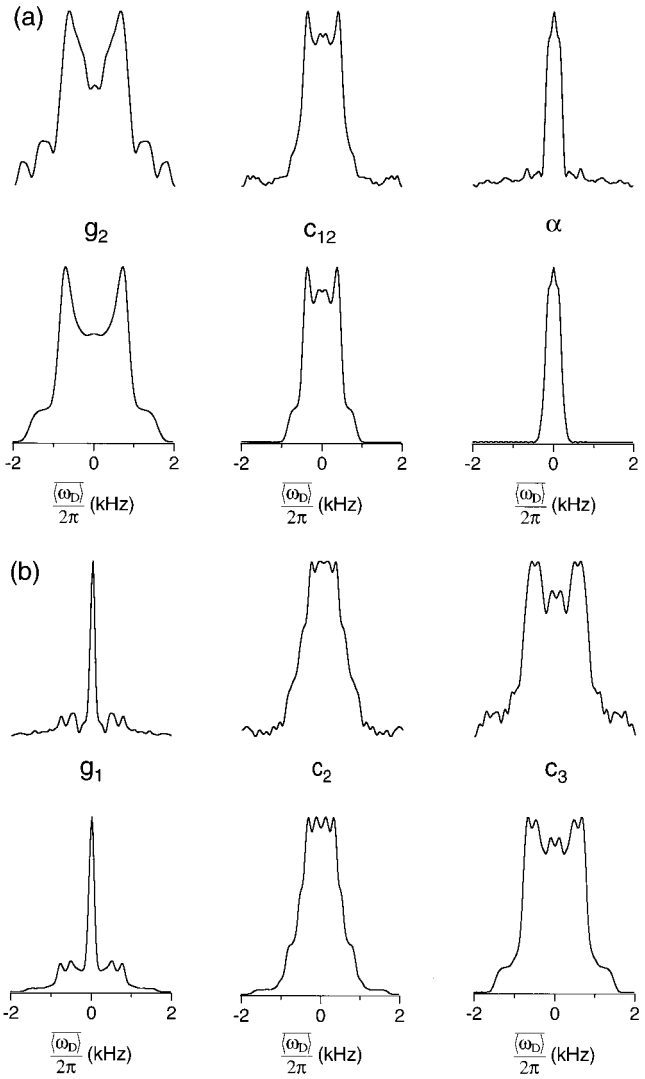

Figure 4. Selected $^{13}C-^{1}H$ dipolar slices from the 2D DROSS spectrum (top) compared with numerical simulations (bottom) for g_2, C_{12}, and α (a) and g_1, C_2, and C_3 (b). The dipolar couplings that generated the best fit between simulation and experimental data are selected for the calculation of the $^{13}C-^{1}H$ segmental order parameter S_{CH}, as described in the text. In (a) input values for $\langle b_{CH}\rangle$ are the following; g_2, 4.1 kHz; C_{12}, 2.2 and 0.7 kHz; and α, 0.9 and 0.2 kHz. ^{1}H resonance offsets for g_2, C_{12}, and α were 0.88, -0.70, and 0.48 kHz while those for ^{13}C were 1.90, -2.90, and 0.75 kHz, respectively. In (b) input values for $\langle b_{CH}\rangle$ are the following: g_1, 0.2, 2.8, and 4.2 kHz; C_2, 0.8, 1.9, 2.8, and 4.4 kHz; and C_3, 0.7, 2.6, and 3.8 kHz. ^{1}H resonance offsets for g_1, C_2, and C_3 were 0.44, -0.30, and -0.64 kHz while those for ^{13}C were 1.10, -2.00, and -2.70 kHz. Values for the ^{13}C CSA tensor corresponding to δ_{11}, δ_{22}, and δ_{33} were taken to be 50, 37, and 13 ppm, respectively, while the ^{1}H CSA was taken to be zero. The timings for τ_1 and τ_2 were those given in Figure 3 for $\chi = 0.393$ and $\epsilon = 0.0$.

axis and the internuclear vector is close to the magic-angle. ^{2}H NMR with a specifically labeled CH_2 group at g_1 results in an intense and narrow line shape superimposed with a broad Pake pattern.[45] Likewise, this inequivalence is observed in the 2D DROSS "slice" taken at the g_1 resonance (see Figure 4b). In this case the origin of the additional splitting, not predicted by ^{2}H NMR, is unkown. Moreover, it is known from ^{2}H NMR that the C_2 segment exhibits three splittings: the sn-2 chain contains two inequivalent CD segments while those found on

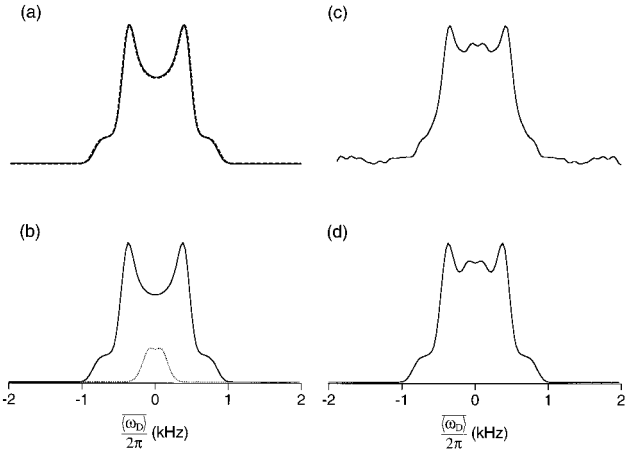

Figure 5. Numerical line shape simulations of DROSS recoupling for the C_{12} site using spectral parameters found in Figure 4 except the CH_2 group was simulated with a motionally averaged $^{1}H-^{1}H$ dipolar coupling of 5.0 kHz. (a) Solid line: finite π pulse widths of 8.8 μs. Dashed line: δ-function π pulses. (b) Overlay of finite pulse simulations for C_{12} and a weighted long-range dipolar coupling with $\langle b_{CH}\rangle$ of 2.2 and 0.7 kHz, respectively. (c) Experimentally obtained line shape for C_{12}. (d) Addition of spectra found in (b).

the chain attached at the g_1 position are degenerate.[46] These inequivalences are also observed in the 2D DROSS experiment. The observed line shapes depicted in Figure 4 are fitted excellently using the motionally averaged $^{13}C-^{1}H$ dipolar couplings corresponding to the order parameters given by ^{2}H NMR while the additional splittings are simulated under the assumption of long-range dipolar interactions.

Long-range couplings which are not predicted by ^{2}H NMR are found in the 2D DROSS experiment due to the fact that the quadrupolar coupling reports on local order whereas $^{13}C-^{1}H$ dipolar couplings may report on larger spatial scales. For example, the small central splittings, observable in most of the recoupled dipolar line shapes, are attributed to dipolar interactions between ^{13}C and a remote ^{1}H and are not due to pulse imperfections. Figure 5a illustrates numerical line shape simulations of the scaled Pake pattern obtained for two motionally equivalent CH segments of the CH_2 group found at the C_{12} position of DMPC under conditions of δ-function pulses (ideal recoupling) superimposed with the line shape obtained with the finite pulse lengths employed in this study. Note that the line shapes are identical. The central splitting found in the experimental line shape is fitted nicely by weighting and coadding the results of Figure 5a with the simulation of a long-range $^{13}C-^{1}H$ dipolar coupling between C_{12} and a remote proton (see Figure 5b). There is excellent agreement between the composite line shape and experimental results (see Figure 5, parts c and d). Similar long-range splittings have been observed in switched-angle spinning experiments that allow evolution of ^{1}H transverse magnetization under recoupled $^{13}C-^{1}H$ dipolar interactions followed by CP to ^{13}C for detection.[29] It is known that in these experiments there is an increase in intensity of the central splitting with increasing CP contact time. For the case of 2D DROSS where rotor-synchronized refocused-INEPT achieves the coherence transfer between ^{1}H and ^{13}C, variation of the transfer delays δ_1 and δ_2 produces a variation of the central splitting intensity corroborating the aforementioned results (data not shown). Presumably, the ^{1}H magnetization of a remote spin evolves under a long range dipolar coupling and is transferred via long-range heteronuclear J coupling to ^{13}C. Long-range dipolar couplings have been employed to yield additional constraints for average conformation in lipid bilay-

(45) Gally, H. U.; Pluschke, G.; Overath, P.; Seelig, J. *Biochemistry* **1981**, *20*, 1826−1831.

(46) Seelig, A.; Seelig, J. *Biochim. Biophys. Acta* **1975**, *406*, 1−5.

ers.[47] Therefore, methods that assign these interactions to a specific ^{1}H would be useful and may include either selective excitation or the addition of a third dimension to the 2D DROSS experiment allowing for ^{1}H chemical shift evolution.

Line shapes corresponding to directly bonded CH pairs are also simulated by weighting and coadding powder patterns obtained from individual simulations following the procedure outlined in Figure 5. The addition of line shapes is justified within the approximation of δ-function pulses and an effectively inhomogeneous Hamiltonian while the weighting factors are chosen to fit the intensities corresponding to the relative transfer effeciency through rotor-synchronized refocused-INEPT. This procedure is particularly convenient for the simulation of inequivalent couplings found at CH_2 segments such as C_2. The ^{13}C$-^1$H dipolar coupling that produces the best fit between simulated and experimentally determined powder patterns is divided by the corresponding rigid lattice dipolar coupling to obtain S_{CH}. The value for the rigid lattice dipolar coupling between a directly bonded CH pair is chosen to be 20.2 kHz which is smaller than the value of 22.7 kHz given by an internuclear distance of 1.11 Å from neutron diffraction data.[48] This choice is justified by measurements of dipolar couplings in small molecules in the solid state, such as calcium formate, which indicate such a departure and are consistent with vibrational averaging of the dipolar interactions.[11] The apparent discrepancy between internuclear distances obtained by neutron diffraction and solid-state NMR is attributed to different time scales of measurement and has been discussed previously.[49] Interestingly, both experimental[12] and theoretical[50] studies on larger molecules such as polymers and long chain hydrocarbons have indicated a more severe vibrational averaging of ^{13}C$-^1$H dipolar interactions in the solid state which is attributed to the increased number of wagging or librational modes. Nevertheless, comparison of S_{CH}, obtained from directly bonded ^{13}C$-^1$H dipolar couplings, with the ^{2}H order parameter S_{CD} indicates good agreement between results obtained from the 2D DROSS technique and ^{2}H NMR (see Table 1). Values of S_{CH} obtained from switched-angle spinning experiments are tabulated for a comparison of the relative accuracy of the techniques.

Considerations affecting the overall sensitivity of the experiment include the coherence transfer from ^{1}H to ^{13}C. It is well-known that ^{1}H$-^{13}$C CP/MAS intensities become sensitive to Hartmann−Hahn mismatch when spinning speeds exceed the strength of the relevant dipolar couplings.[51] Experiments in our lab on fluid phase lipids indicate that ^{1}H$-^{13}$C CP/MAS intensities are sensitive to Hartmann−Hahn mismatch even at moderate spinning speeds. This is due to the fact that dipolar couplings in fluid phase lipids are reduced significantly by motional averaging and that the Hamiltonian is rendered inhomogeneous due to fast limit axial diffusion, so that optimal CP intensities are difficult to achieve and maintain for long times. Typically this problem is rectified by employing any of a wealth of the new phase-switched and amplitude-modulated techniques;[52−56] however, for inhomogeneous systems, these schemes generate an orientation-dependent polarization transfer which may complicate the interpretation of powder line shapes. Consequently, we have chosen rotor-synchronized refocused-INEPT in order to ensure an orientation independent transfer through the scalar coupling so that powder line shapes are determined solely by the evolution under H^{eff} (see eq 2) during t_1. The utility of an orientation-independent transfer is exhibited by the sharp CH line shape visible for the g_1 site expected from ^{2}H NMR and arising from a bond oriented at the magic-angle which was lost in previously published spectra for which CP was used (see Figure 4b).[29,57] This approach is well suited for fluid phase lipids since the ^{1}H and ^{13}C line widths are less than J_{CH}. For systems where transverse relaxation rates are rapid relative to J_{CH}, the sensitivity of the 2D DROSS experiment will be compromised since the time scale of the refocused-INEPT transfer is approximately $^1/_2J_{CH}$.[40] In this case, CP transfer schemes may offer a sensitivity advantage, and dipolar couplings may be extracted by incorporating the particular CP transfer scheme into the line shape simulations.

Figure 6 depicts the normalized ^{13}C resonance intensity as a function of evolution period, t_1, along with the corresponding Fourier transform for selected ^{13}C resonances in DMPC obtained with the S-DROSS sequence where $\chi = 0.393$ and $\epsilon = 0$. The fact that values of τ_1 and τ_2 may be chosen so that $\epsilon = 0$ presents two advantages over experiments which require switched-angle spinning,[29,30] one being the ability to determine the sign of the dipolar interaction independently from the ratio $\chi\langle\pm\omega_D\rangle/\pi J_{CH}$ and the other being the ability to do so unambiguously with only one set of scale factors. These advantages stem from the fact that, in the switched-angle spinning experiment, the sign of the dipolar interaction in given by the sign of $\langle\pm\omega_D\rangle P_2(\cos\Theta) + \pi J_{CH}$ while in the case of S-DROSS the sign is given by $\chi\langle\pm\omega_D\rangle + \epsilon\pi J_{CH}$.

Table 1. Comparison of S_{CH} with S_{CD} for DMPC at 30 °C

carbon position	S_{CH} (±0.02)[a]	S_{CH}[b]	$\lvert S_{CD}\rvert$[c]
13	−0.09	ND	0.10[d]
12	−0.11	ND	0.14[e]
3	−0.13	ND	0.18[f]
	−0.19	−0.22 ± 0.03	0.21[f]
2	−0.09	ND	0.09[f]
	−0.14	−0.12 ± 0.03	0.15[f]
	−0.21	−0.21 ± 0.03	0.21[f]
g_1	0.00	ND	0.00[g]
	−0.15	−0.12 ± 0.04	0.16[g]
g_2	−0.20	−0.16 ± 0.04	0.19[g]
g_3	−0.23	−0.19 ± 0.03	0.21[g]
a	+0.04	+0.04 ± 0.02	0.05[h]
b	−0.03	−0.04 ± 0.02	0.04[h]

[a] S_{CH} is defined as the ratio of the motionally averaged dipolar splitting, $\langle b_{CH}\rangle$, divided by the rigid lattice value taken to be 20.2 kHz for a directly bonded ^{13}C$-^1$H pair. [b] S_{CH} for egg yolk lecithin taken from Hong et al. (Hong, M.; Schmidt-Rohr, K.; Pines, A. *J. Am. Chem. Soc.* **1995**, *117*, 3310−3311), where the rigid lattice dipolar coupling is taken to be 22.7 kHz for a directly bonded ^{13}C$-^1$H pair. [c] S_{CD} is defined as the ratio of the motionally averaged quadrupolar splitting $\langle\Delta\nu_Q\rangle$, divided by the rigid lattice value taken to be 127 kHz. [d] Interpolated between 23 and 40 °C from values given in: Trouard, T. P.; Alam, T. M.; Zajicek, J.; Brown, M. F. *Chem. Phys. Lett.* **1992**, *189*, 67. Meier, P.; Ohmes, E.; Kothe, G. *J. Chem. Phys.* **1986**, *85*, 3598. [e] Oldfield, E.; Meadows, M.; Jacobs, R. *Biochemistry* **1978**, *17*, 2727. [f] Seelig, A.; Seelig, J. *Biochemistry* **1974**, *13*, 4839. [g] Gally, H. U.; Pluschke, G.; Overath, P.; Seelig, J. *Biochemistry* **1981**, *20*, 1826. [h] Gally, H. U.; Niederberger, W.; Seelig, J. *Biochemistry* **1975**, *14*, 3647.

(47) Hong, M.; Schmidt-Rohr, K.; Zimmermann, H. *Biochemistry* **1996**, *35*, 8335−8341.
(48) Al-Karaghouli, A. R.; Koetzle, T. F. *Acta Crystallogr.* **1975**, *B31*, 2461−2465.
(49) Roberts, J. E.; Harbison, G. S.; Munowitz, M. G.; Herzfeld, J.; Griffin, R. G. *J. Am. Chem. Soc.* **1987**, *109*, 4163−4169.
(50) Henry, E. R.; Szabo, A. *J. Chem. Phys.* **1985**, *82*, 4753−4761.
(51) Stejskal, E. O.; Schaefer, J.; Waugh, J. S. *J. Magn. Reson.* **1977**, *28*, 105−112.
(52) Wu, X.; Zilm, K. W. *J. Magn. Reson. A* **1993**, *104*, 154−165.
(53) Peerson, O. B.; Wu, X.; Kustanovich, I.; Smith, S. O. *J. Magn. Reson. A* **1993**, *104*, 334−339.
(54) Hediger, S.; Meier, B. H.; Ernst, R. R. *Chem. Phys. Lett.* **1993**, *213*, 627−635.
(55) Metz, G.; Wu, X.; Smith, S. O. *J. Magn. Reson.* **1994**, *A110*, 219−227.
(56) Sun, B. Q.; Costa, P. R.; Griffin, R. G. *J. Magn. Reson. A* **1995**, *112*, 283−288.
(57) Hong, M.; Schmidt-Rohr, K.; Nanz, D. *Biophys. J.* **1995**, *69*, 1939−1950.

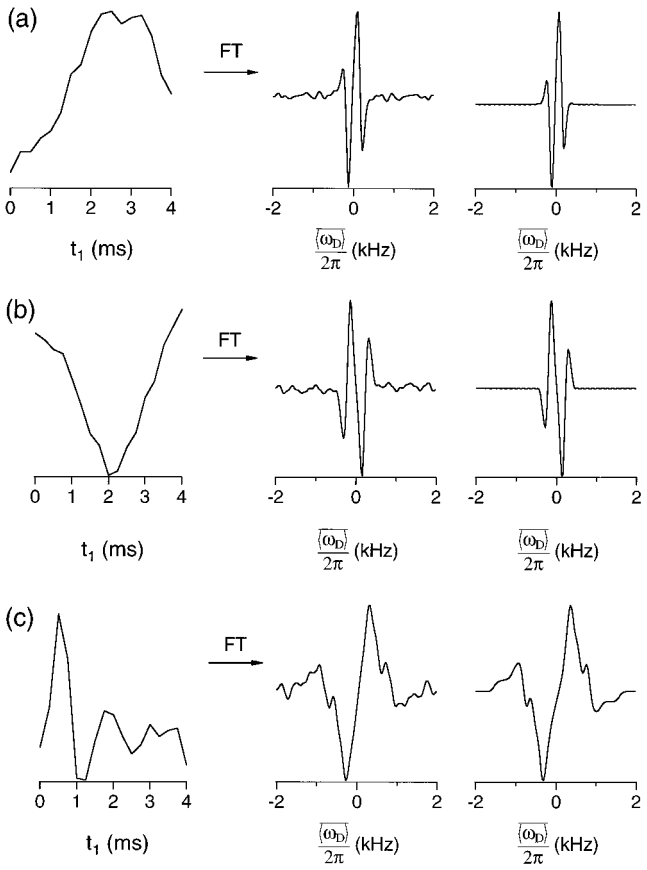

Figure 6. S-DROSS experimental data and numerical line shape simulations for β, α, and C_2 sites depicted in a−c, respectively. From left to right, the buildup of ^{1}H antiphase magnetization monitored by ^{13}C detection is depicted followed by the corresponding Fourier transform and numerical line shape simulations. Input parameters for the simulations are as follows: (a) $\langle b_{CH}\rangle = +0.6$ kHz with ^{1}H and ^{13}C resonance offsets of 0.22 and 2.20 kHz; (b) $\langle b_{CH}\rangle = -0.9$ kHz with ^{1}H and ^{13}C resonance offsets of 0.47 and 1.60 kHz; and (c) $\langle b_{CH}\rangle = +1.9$, $+2.8$, and $+4.4$ kHz with ^{1}H and ^{13}C resonance offsets of -0.30 and -1.00 kHz. The timings for τ_1 and τ_2 were those given in Figure 2 for $\chi = 0.393$ and $\epsilon = 0.0$.

For ^{13}C sites containing degenerate ^{13}C−^{1}H dipolar couplings, the sign of the dipolar coupling is easily obtained from the initial buildup rate of antiphase magnetization provided that $|\chi\langle\pm\omega_D\rangle| \gg \epsilon\pi J_{CH}$ as is the case here since $\epsilon = 0$. For example, the buildup curves for β and α positions indicate positive and negative dipolar couplings, respectively. The negative dipolar coupling, or positive order parameter, found at the α position is consistent with the fact that the choline head group makes an unusual bend at the phosphate junction.[47,58] In contrast, segments that contain non-degenerate ^{13}C−^{1}H dipolar couplings may complicate the time-domain analysis. In this case, Fourier transformation of the data would clarify the results as inequivalent couplings would manifest as separate antiphase Pake doublets with sign differences given by opposite polarity since a positive dipolar coupling gives rise to a $+-+-$ intensity pattern while the negative coupling yields a $-+-+$ pattern (see Figure 6, parts a and b). Just as in the DROSS experiment, non-degenerate ^{13}C−^{1}H dipolar couplings may be simulated as a superposition of Pake patterns. In Figure 6c, all of the inequivalent couplings found at C_2 are found to be positive using this approach. A summary of the signs of ^{13}C−^{1}H dipolar interactions measured with S-DROSS utilizing either the time or frequency domain analysis is given in Table 1 and is in agreement with previous studies.[29,57]

The magnitudes and signs of ^{13}C−^{1}H dipolar couplings determined in this study are useful for determining average molecular conformation. In the order matrix approach, each CH segment generally requires at least five anisotropies to be measured so that the complete orientation of the segmental order tensor may be specified.[59] The elements of the complete order matrix furnish angular distribution functions that yield the average orientation of a CH segment with respect to the director axis.[60−62] Alternatively, methods that involve the fitting of motionally averaged powder line shapes with either assumed or known dynamical models may provide more insight between fast limit molecular dynamics and motionally averaged tensors.[6] Other approaches, utilizing motionally averaged dipolar couplings and *J* couplings in conjunction with molecular dynamics simulations, are also a promising means for determining average molecular structure.[63]

Conclusions

We have presented an alternative method for the measurement of the magnitudes and signs of ^{13}C−^{1}H dipolar couplings in liquid crystalline systems such as lipid bilayers. It is possible to obtain information regarding the average orientation of CH bond segments without recourse to isotopic enrichment. Implementation of the proposed experiments is straightforward in that they do not require specialized hardware for angle switching between the evolution and detection periods. The techniques are applicable for systems where molecular motions render the ^{1}H spin dynamics effectively inhomogeneous at experimentally realizable spinning speeds.

We anticipate that, in the future, the information provided by dipolar recoupling, combined with MAS techniques which simultaneously correlate chemical shifts and long-range scalar couplings, will provide important constraints for determining the average molecular conformation in lipid bilayers. In addition, it may be possible to incorporate an inversion recovery period in the 2D DROSS experiment as a probe for anisotropic ^{13}C spin−lattice relaxation. Presumably, recoupled dipolar powder patterns would serve as a reporter of orientation-dependent relaxation which would present the exciting possibility of directly probing the rates of dynamic processes through dipolar recoupling.

Acknowledgment. The authors would like to thank Drs. P. R. Costa and G. Wu for many stimulating discussions and a critical reading of the manuscript. Thanks are also accorded to Dr. A. E. Bennett, who generously provided the spin dynamics simulation program used in this study. This research was supported by grants from the National Institutes of Health (GM-25505, GM-23289, and RR-00995).

JA962951B

(58) Bueldt, G.; Gally, H. U.; Seelig, J.; Zaccai, G. *Nature* **1978**, *271*, 182−184.

(59) Saupe, A. *Z. Naturforsh.* **1964**, *19a*, 161−171.

(60) Hentschel, R.; Schlitter, J.; Sillescu, H.; Spiess, H. W. *J. Chem. Phys.* **1978**, *68*, 56.

(61) Torchia, D. A.; Szabo, A. *J. Magn. Reson.* **1985**, *64*, 135−141.

(62) Schmidt-Rohr, K.; Hong, M. *J. Phys. Chem.* **1996**, *100*, 3861−3866.

(63) Howard, K. P.; Prestegard, J. H. *J. Am. Chem. Soc.* **1995**, *117*, 5031−5040.